ADVANCED FUNCTIONAL MATERIALS
www.afm-journal.de

Bright Blue Solution Processed Triple-Layer Polymer Light-Emitting Diodes Realized by Thermal Layer Stabilization and Orthogonal Solvents

Roman Trattnig, Leonid Pevzner, Monika Jäger, Raphael Schlesinger, Marco Vittorio Nardi, Giovanni Ligorio, Christos Christodoulou, Norbert Koch, Martin Baumgarten, Klaus Müllen, and Emil J. W. List**

The realization of fully solution processed multilayer polymer light-emitting diodes (PLEDs) constitutes the pivotal point to push PLED technology to its full potential. Herein, a fully solution processed triple-layer PLED realized by combining two different deposition strategies is presented. The approach allows a successive deposition of more than two polymeric layers without extensively redissolving already present layers. For that purpose, a poly(9,9-dioctyl-fluorene-co-N-(4-butylphenyl)-diphenylamine) (TFB) layer is stabilized by a hard-bake process as hole transport layer on top of poly(3,4-ethylenedioxythiophene):poly(styrenesulfonate) (PEDOT:PSS). As emitting layer, a deep blue emitting pyrene-triphenylamine copolymer is deposited from toluene solution. To complete the device assembly 9,9-bis(3-(5′,6′-bis(4-(polyethylene glycol)phenyl)-[1,1′:4′,1″-terphenyl]-2′-yl)propyl)-9′,9′-dioctyl-2,7-polyfluorene (PEGPF), a novel polyfluorene-type polymer with polar sidechains, which acts as the electron transport layer, is deposited from methanol in an orthogonal solvent approach. Atomic force microscopy verifies that all deposited layers stay perfectly intact with respect to morphology and layer thickness upon multiple solvent treatments. Photoelectron spectroscopy reveals that the offsets of the respective frontier energy levels at the individual polymer interfaces lead to a charge carrier confinement in the emitting layer, thus enhancing the exciton formation probability in the device stack. The solution processed PLED-stack exhibits bright blue light emission with a maximum luminance of 16 540 cd m^{-2} and a maximum device efficiency of 1.42 cd A^{-1}, which denotes a five-fold increase compared to corresponding single-layer devices and demonstrates the potential of the presented concept.

1. Introduction

One of the key advantages of polymer light-emitting devices (PLEDs) can be found in their potential to be assembled completely by solution-based processes, which in principle allow high throughput, low-cost fabrication of large area displays and lighting applications. Yet, to extend solution processed PLED technology from lab-[1] to full production scale, significant improvements in the material performance have to be devised. In addition, it is necessary to adapt material and device concepts to solution- based roll-to-roll fabrication processes. Only if similar performance values as achieved for organic light-emitting devices (OLEDs) fabricated based on high-vacuum vapor deposition techniques can be realized, the benefit of cost effective and high throughput fabrication based on solution processing can reach its full potential for large area (flexible) devices,[2] signage[3] and lighting applications.[4]

Yet, to achieve the necessary requirements of high brightness values in the device, alongside with high efficiency and stable operation, OLEDs require balanced charge carrier injection and charge carrier

R. Trattnig, M. Jäger, Prof. E. J. W. List
NanoTecCenter Weiz Forschungsgesellschaft mbH
Franz Pichler Straße 32, A-8160 Weiz, Austria
E-mail: emil.list@ntc-weiz.at
L. Pevzner, Prof. M. Baumgarten, Prof. K. Müllen
Max-Planck-Institut für Polymerforschung
Ackermannweg 10, D-55128 Mainz, Germany
E-mail: muellen@mpip-mainz.mpg.de
R. Schlesinger, Dr. M. V. Nardi, G. Ligorio, C. Christodoulou, Prof. N. Koch
Institut für Physik
Humboldt-Universität zu Berlin
Brook-Taylor-Strasse 6, D-12489 Berlin, Germany
Prof. N. Koch
Helmholtz Zentrum Berlin für Materialien und Energie GmbH
Elektronenspeicherring BESSY II
Albert-Einstein-Strasse 15, D-12489 Berlin, Germany
Prof. E. J. W. List
Institut für Festkörperphysik
Graz University of Technology
Petersgasse 16, A-8010 Graz, Austria

DOI: 10.1002/adfm.201300360

transport[5] as typically realized only in multilayer device structures. The main objectives for such multilayer structures are, firstly, to provide an efficient injection and transport of positive (holes) and negative (electrons) charge carriers drifting/diffusing from the electrodes to the emitting layer (EML) and, secondly, to block flowing of charges out of the EML without formation of excitons, i.e., confining charge carriers within the EML for enhanced exciton formation probability. For OLEDs based on small molecules defined multilayer structures can easily be realized using vacuum vapor deposition techniques. However, because of the cost intensive equipment, the high material waste in the production process and the slow processing speed, there is a huge barrier to bring devices produced in that manner to industrial mass production. Additionally, many small molecular materials show a potential drawback of changes in morphology caused by recrystallization or molecular migration at elevated temperature during operation or even at room temperature.[6,7] A different and cost-effective approach allowing large area production is to apply organic materials (polymers and small molecules) by solution-based processes like inkjet-printing or slot-dye roll-to-roll processing. While the issues concerning changes in morphology still exist for soluble small molecules, polymers comprise an even better alternative. Polymers can exhibit good film formation properties upon solution processing, high morphological stability and a higher resistance to molecular diffusion than small molecules.[8]

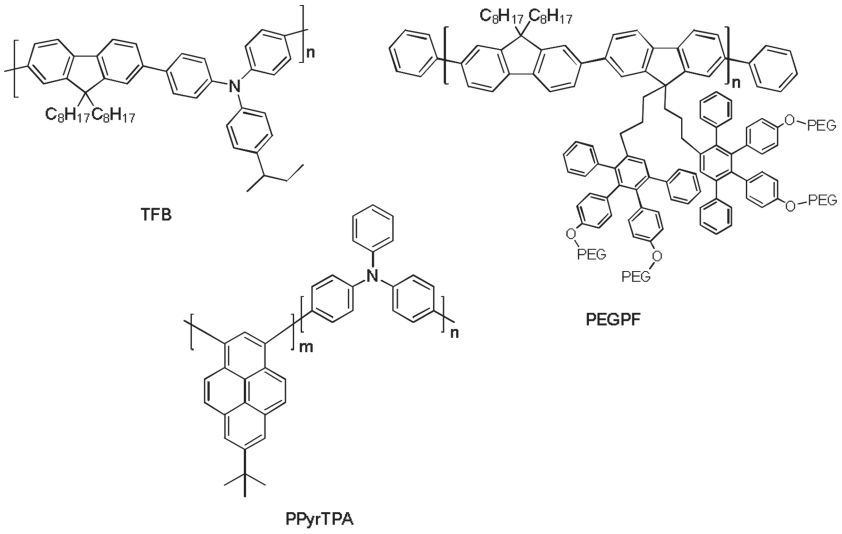

Figure 1. Chemical structures of the polymers used to realize the fully solution processed triple-layer PLED assembly: TFB (top left), PEGPF (top right) and PPyrTPA (bottom).

To implement multilayer device structures by subsequent solution processing of different layers, care has to be taken by the selection of solvents and materials to ensure that upon deposition of the sequent material the preceding layer does not redissolve. Different approaches addressing this issue were already presented and are based mostly on crosslinking reactions,[9–11] use of orthogonal solvents,[12,13] a layer-stabilizing "hard-bake" process[14] or on liquid buffer layers in between when applying the subsequent polymer layer.[15]

In this contribution we report on a fully solution processed triple-layer PLED assembly that combines a hard–bake process, to insolubilize the bottom hole transporting layer (HTL), and the deposition of polymers from orthogonal solvents for both the emissive layer (EML) and the electron transport layer (ETL). For the single layer, as well as for all multilayer devices, the previously introduced pyrene-triphenylamine copolymer PPyrTPA (**Figure 1**) is used as the emitting material.[16] PPyrTPA shows a deep blue electroluminescence (EL) emission and high photoluminescence quantum yield. Furthermore, in contrast to well-established blue emitting materials like fluorene-[17,18] or indenofluorene based polymers[19–21] which tend to suffer from discoloration due to material degradation as a consequence of an intrinsic weakness of these polymers at the 9-position of the fluorene unit,[22–24] PPyrTPA exhibits extraordinary chemical as well as spectral stability during operation.[16,25] For a bilayer device with enhanced hole injection properties, poly(9,9-dioctyl-fluorene-co-N-(4-butylphenyl)-diphenylamine) (TFB, Figure 1) acts as hole injecting and transporting material at the anode side of the emissive layer. TFB is known as a high mobility hole transport polymer[26] forming smooth and insoluble layers with a thickness of only a few nanometers, when heated at temperatures between 180–200 °C and spin-rinsed afterwards.[14] In a last step, the TFB/PPyrTPA assembly is completed by an electron transporting and hole blocking layer at the cathode side of the EML, forming the triple-layer device. This ETL comprises a properly tuned polyfluorene polymer (PEGPF, Figure 1). PEGPF bears poly(ethylene glycol) (PEG) side chains, which ensure the solubility of the material in polar solvents like methanol, thus preventing an intermixing with PPyrTPA during the deposition process of the ETL. Furthermore, PEGPF provides the advantages of PEG as electron injection material[27] and surfactant[28] with the conducting properties of the conjugated polyfluorene, which compensates for the insulating properties of PEG when the layer thickness is not controlled properly.[29] The implementation of two different solution–based multilayer approaches, based on orthogonal solvents and thermal stabilization of a polymeric layer, for several sequential spin-coating and annealing steps without harming the preceding layer is proven by atomic force microscopy (AFM) investigations. Ultraviolet photoemission spectroscopy (UPS) measurements evidence that the combination of materials and their assembly in PLEDs, as presented in this work, exhibit a favorable energy level alignment, i.e., efficient electron blocking at the HTL/EML-interface and hole blocking at the EML/ETL-interface. This allows good charge carrier confinement within the EML, resulting in an enhancement of the maximum luminance and electroluminescence efficiency for multilayer PLEDs in comparison to single layer devices. Furthermore, the magnitude of the improvement is in the same range as for previously reported works on PLEDs with an assembly based on polar soluble polyfluorene,[13] thermally crosslinked[30–32] or thermally stabilized polymer interlayers.[14,15]

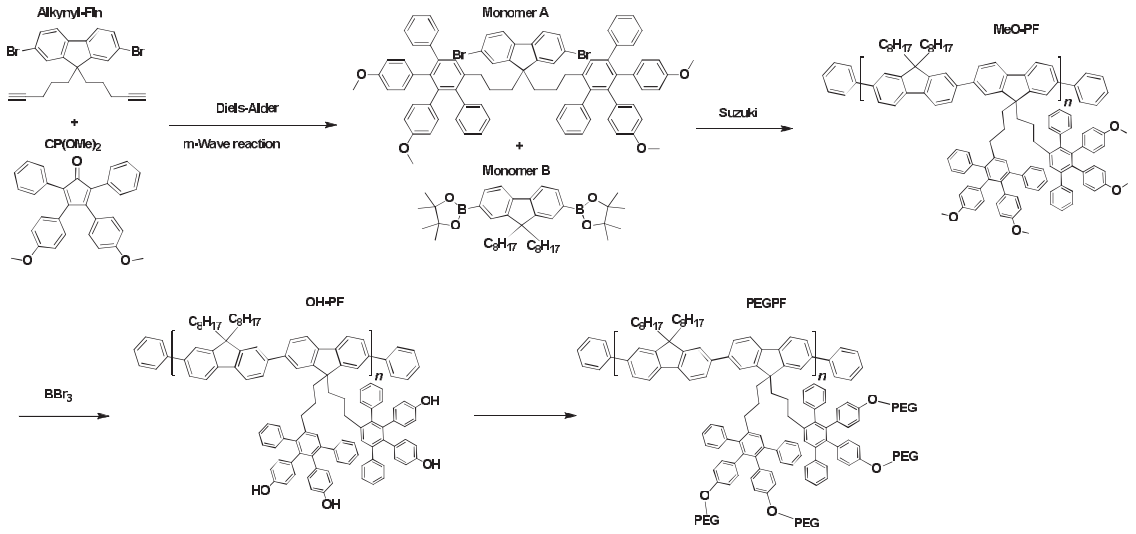

Figure 2. Scheme of the synthesis of the polar soluble PEGylated polyfluorene PEGPF.

2. Results and Discussion

2.1. Synthesis of PEGPF

Polar soluble polyfluorenes (PF) for orthogonal processing have been previously reported by our group.[13] We have synthesized a new polar PF in which the attachment of PEG sidegroups (PEGylation) is carried out in the last step, thereby allowing to overcome the limitations to the applicability of this process and especially to the reproducibility of the molecular weight (**Figure 2**). Since the Suzuki polycondensation is a step-growth polymerization technique, the use of equimolar amounts of both monomers is crucial to obtain high conversion and thus high molecular weight polymers. However, the PEGylated monomer used for the synthesis of the previously reported polar soluble PF was polydisperse due to the intrinsic polydispersity of the PEG chains. Additionally, the monomers are waxy, hygroscopic substances and thus hard to handle. These issues limited the accuracy of the initial weight and often led to low molecular weight polymers. By using the synthetic route presented in the current work, we were able to considerably lower the reaction time of the Suzuki polycondensation to less than 1 day in comparison to the very slowly proceeding process (reaction time ≈6 days) reported earlier.[13]

In our new approach, a polar soluble PF has been developed where the PEG chains were introduced in a polymer-analogous reaction. Monomer A was synthesized in a microwave assisted Diels-Alder cycloaddition from an alkynyl functionalized 2,7-dibromofluorene (Alkynyl-Fln) and the doubly methoxy functionalized tetraphenylcyclopentadienone $CP(OMe)_2$. The comonomer B was necessary to lower the steric hindrance during the polymerization and to prevent aggregation on a later stage. The alternating copolymer MeO-PF was obtained with reproducible molecular weights (M_n > 15 000 g mol^{-1}) by Suzuki polycondensation and subsequent endcapping. The freshly prepared MeO-PF was readily soluble in tetrahydrofuran (THF), toluene and chlorinated solvents and showed a low tendency to aggregate due to the strong shielding of the PF main chain by the large, stiff polyphenylene-dendrons of the side chains.[33] In the next step, the methoxy groups were cleaved using BBr_3 solution yielding a hydroxyl functionalized polyfluorene (OH-PF) which can be used for further functionalization (e.g., grafting). Despite its highly amphiphilic character, OH-PF was soluble in THF which is attributed to the large steric demand of the side chains.[33] OH-PF was PEGylated using PEG750-Br (endcapped with methoxy and bromine). The degree of functionalization was proven by ^{1}H-NMR to be nearly quantitative (not shown). The number average molecular weight exceeded 48 000 g mol^{-1}, depending on the size of the core PF. PEGPF proved to be soluble in methanol and ethanol in addition to the typical solvents used for PF. Unlike most amphiphilic PF, PEGPF does not aggregate in solution in concentrations as high as 1 g L^{-1} over at least a month. A low tendency to aggregate is a crucial property for thin film device applications.

Hence, based on its good solubility in methanol and ethanol and due to its film formation properties, PEGPF presents an attractive material for solution processed multilayer PLEDs. In particular, not redissolving it facilitates the deposition of an additional layer by spin coating on top of a preceding material like PPyrTPA, which is soluble primarily in non-polar solvents.

2.2. Morphological Stability of Solution Processed Polymeric Layers

The realization of multilayer assemblies by thermal treatment or by the utilization of orthogonal solvents has already been presented in previous work.[12,14] Nonetheless, especially for the latter approach it is essential to assess the particular processes assiduously, since adverse effects like reduced wettability can easily occur, caused by the difference in the polarity of the layer and the coating solution.[34] Thus, the film formation properties (film thickness and surface morphology) of TFB, PPyrTPA and PEGPF in multilayer assemblies were investigated by AFM. At first, poly(3,4-ethylenedioxythiophene):poly styrenesulfonate (PEDOT:PSS) was deposited onto indium tin

oxide (ITO)-covered glass-substrates. ITO has a rough and spiky surface (**Figure 3**a) which is strongly smoothed by PEDOT:PSS (Figure 3b). As the second layer TFB was spin cast onto PEDOT:PSS from xylene solution, annealed at high temperature (200 °C) and spin rinsed with pure toluene to remove any soluble portion of TFB. Upon further spin rinsing treatments with pure solvent, however, no morphological changes or polymer dissolution could be detected by AFM. This confirms the stability of the thermally treated layer (Figure 3c). As the next step PPyrTPA was deposited from a toluene solution. To reduce possible wettability issues, prior to the deposition of the next layer, PPyrTPA substrates were spin rinsed with pure methanol. AFM demonstrates that PPyrTPA exhibited perfect morphological stability upon this solvent treatment (Figure 3d). As the topmost organic material, PEGPF was deposited from methanol solution forming a smooth layer without wettability issues (Figure 3e). In summary, layer morphologies and stabilities, as confirmed by AFM, reveal that the described combination of a layer stabilizing hard-bake process and an orthogonal solvent approach is well suitable for the targeted solution processed multilayer assembly of TFB, PPyrTPA and PEGPF.

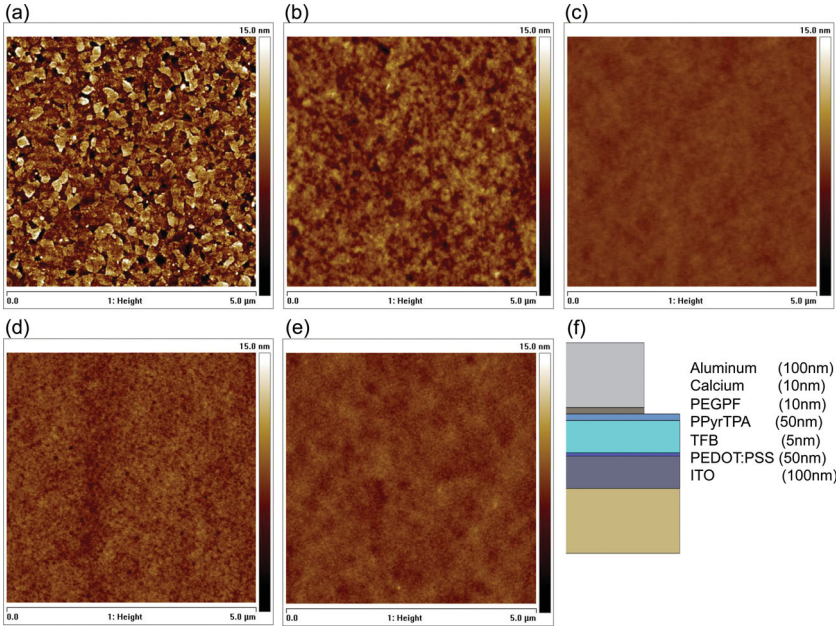

Figure 3. AFM topography images (5 µm × 5 µm) measured in tapping mode of a) ITO, b) PEDOT:PSS, c) TFB, d) PPyrTPA and e) PEGPF. The RMS-surface roughness values are 2.6, 1.2, 0.3, 0.8 and 0.5 nm. f) Scheme of the layer by layer assembly of the PLED-stack. The drawn thicknesses of the individual layers are true to scale.

2.3. Energy-Level Alignment in the Triple-Layer Assembly

Efficient charge carrier injection into as well as their confinement within the EML are decisive for the realization of efficient PLEDs. These properties strongly depend on the frontier energy level offsets at the interfaces. Hence, UPS measurements were conducted in order to assess the interface energetics of the as described assembly. Valence region UPS and secondary electron cutoff (SECO) spectra to measure the work function (φ) and interface dipoles are depicted in **Figure 4**. The photoemission onset of the respective valence bands were determined to be 0.8 eV below the Fermi level (E_F) for TFB, 1.0 eV for PPyrTPA and 1.5 eV for PEGPF. The corresponding ϕ values were 4.5 eV, 4.7 eV and 4.4 eV, respectively. Consequently, the ionization energy (*IE*) values were 5.3 eV for TFB, 5.7 eV for PPyrTPA and 5.9 eV for PEGPF. The valence region spectra of PPyrTPA on TFB show no sign of TFB features and are in good accordance with recently published work on this pyrene-based polymer.[16] The deposition of PEGPF finally suppresses all PPyrTPA features and one broad peak exhibiting a distinct tail towards lower binding energies is observed. X-ray photoelectron spectroscopy (XPS) (Figure S3, Supporting Information) of the layers further corroborates the AFM-results. Complete coverage can be concluded from the fact that elemental core levels specific to the underlying layers were strongly attenuated or vanished completely upon overlayer deposition.

A scheme of the energy level alignment across the PEDOT:PSS/TFB/PPyrTPA/PEGPF interfaces is depicted in **Figure 5**, displaying valence band maximum (VBM) and conduction band minimum (CBM) levels as well as φ, *IE* and estimated electron affinity (*EA*) values. *EA* values were

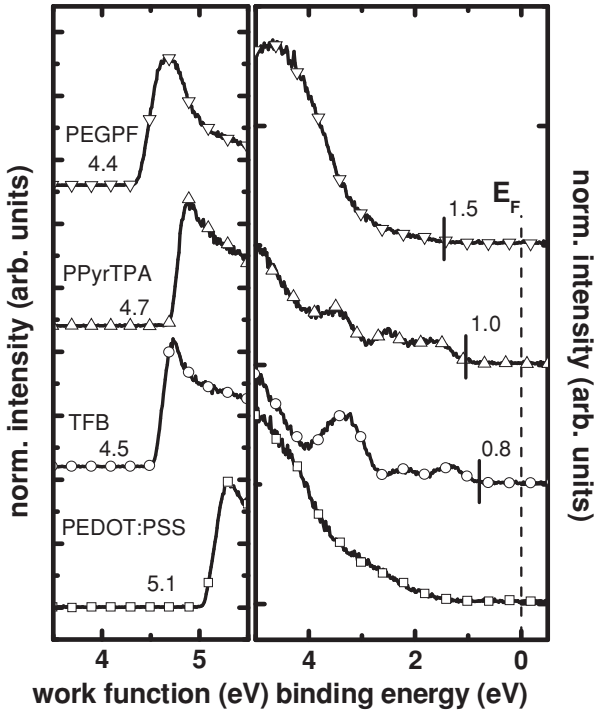

Figure 4. Secondary electron cutoff- (left) and valence region UPS spectra (right) of PEDOT:PSS, TFB, PPyrTPA and of PEGPF in a layer-by-layer assembly. The tick at each spectrum indicates the photoemission onset from the highest occupied level of the respective polymer.

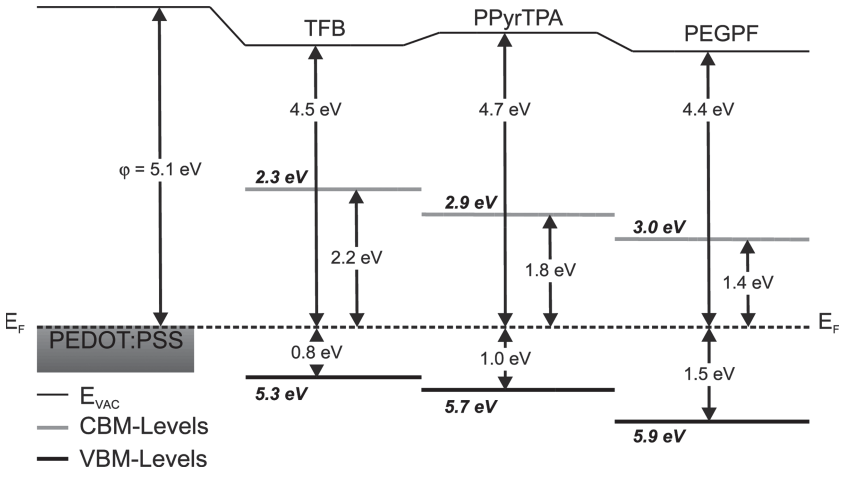

Figure 5. Energy level diagram for a PEDOT:PSS/TFB/PPyrTPA/PEGPF multilayer PLED stack displaying the corresponding VBM and CBM energy levels, *IE* and estimated *EA* (in italics), as well as the workfunction φ.

approximated by $EA = IE - E_g$, where E_g denotes the energy of the optical bandgap derived from the onsets of the particular absorption spectra. As can be seen in Figure 4 and 5 shifts of the vacuum level Δ_{vac} occur between the different layers. The most distinct shift occurs between PEDOT:PSS and TFB where Δ_{vac} is –0.6 eV. According to Hwang et al. interface dipoles, as well as band bending, account for this shift.[35] In addition, Δ_{vac} = 0.2 eV between TFB and PPyrTPA, and Δ_{vac} = –0.3 eV at the PPyrTPA/PEGPF-interface were observed, which are most likely due to a preferential orientation of intra-molecular dipoles at the interfaces.[36] From Figure 5 we deduce that the selected assembly provides the necessary prerequisites for charge carrier confinement in the emissive layer. Between TFB and PPyrTPA, as well as between PPyrTPA and PEGPF, the estimated CBM levels have an offset of 0.4 eV, which are the offsets relevant for electron injection from PEGPF into the EML and extraction from the EML into TFB. The offset for injecting holes from TFB into PPyrTPA (0.2 eV), however, is smaller than the one for extracting them to PEGPF (0.4 eV). As a consequence of these barriers, charge carrier extraction (electrons and holes) from the emitting layer is expected to be significantly constrained compared to PPyrTPA-single layer devices.

2.4. Electroluminescent Properties and Device Performance of Single- and Multilayer PLEDs

For the evaluation of the electroluminescent properties and efficiencies of TFB, PEGPF and PPyrTPA in single-layer PLEDs, devices were fabricated in the standard sandwich structure ITO/PEDOT:PSS/polymer/Ca/Al. The thickness of the emitting layer was 50 nm for all devices and was optimized for PPyrTPA with respect to its luminous efficiency. **Figure 6**a–c presents the current density-voltage-luminescence (J-V-L) characteristics and EL-emission spectra (insets of Figure 6a–c) for the single-layer devices. All relevant device parameters (EL-emission onset, maximum luminance and luminous efficiency (LE)) are listed in **Table 1**. The PLEDs showed a LE between 0.02 cd A^{-1} and 0.27 cd A^{-1} and exhibited deep blue emission, as typical for these materials, which correspond to Commission Internationale de l'Éclairage 1931 (CIE1931) coordinates of x = 0.17, y = 0.10 for TFB, x = 0.16, y = 0.15 for PEGPF and x = 0.16, y = 0.20 for PPyrTPA. The EL-spectra are identical, in terms of shape and position, to the photoluminescence spectra of the particular materials in solid state (Figure S1, Supporting Information). In addition, no difference in the PEGPF emission characteristics was detected, e.g., caused by the polar PEG-sidechains, compared to polyfluorene with non-polar sidechains.[37] Yet, the performance of all single-layer devices was moderate. An unfavorable energy level alignment, forming injection-inhibiting barriers for charge carriers of up to 0.7 eV at the PEDOT:PSS/EML- and/or at the EML/Ca-interface (Figure S2, Supporting Information) is identified as the cause for the low efficiencies.

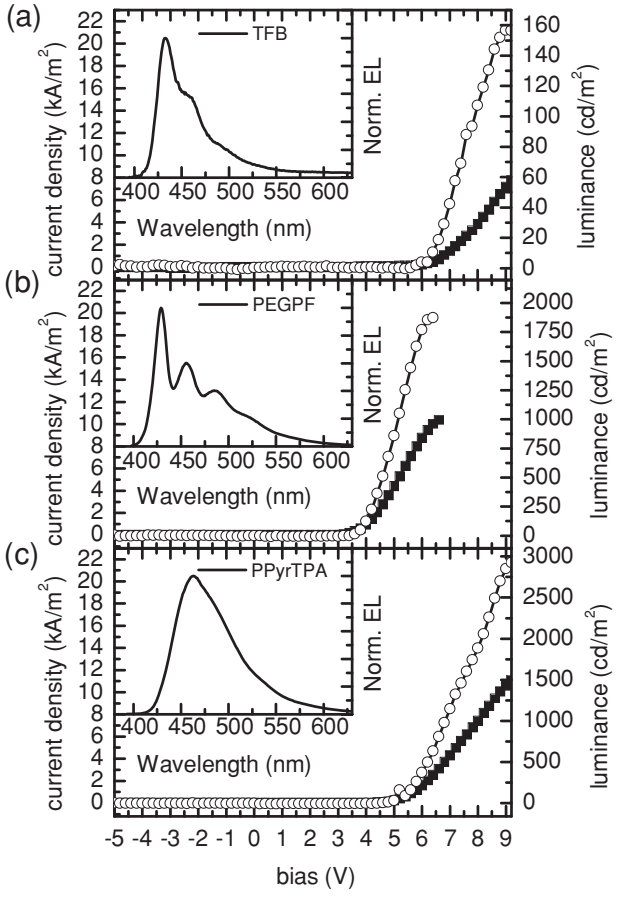

Figure 6. Current density (line with squares)/ luminance (line with circles) as a function of the bias voltage in a) an ITO/PEDOT:PSS/TFB/Ca/Al device, b) an ITO/PEDOT:PSS/PEGPF/Ca/Al device and c) an ITO/PEDOT:PSS/PPyrTPA/Ca/Al device. The insets show the electroluminescence emission spectra of the same devices at a current density of 1.11kA m^{-2} and at a bias around 6.8, 4, and 5.7 V, respectively.

Table 1. Electroluminescent characteristics of investigated single- and bilayer and triple-layer devices.

organic layer geometry	onset voltage [V][a)]	η [cd A^{-1}][b)]	max. luminance [cd m^{-2}]	EL peak [nm][c)]	CIE 1931 coordinates[c)]
TFB	5.7	0.02	157	432	x = 0.173 y = 0.102
PEGPF	3.6	0.2	1872	429	x = 0.164 y = 0.145
PPyrTPA	4.4	0.27	2924	462	x = 0.159 y = 0.197
TFB/PPyrTPA	4.0	0.43	7817	460	x = 0.157 y = 0.174
TFB/ PPyrTPA/ PEGPF	3.9	1.42	16 540	465	x = 0.163 y = 0.216

[a)]Voltage at a luminance of 1 cd m^{-2}; [b)]value of maximum efficiency; [c)]at a current density of 1.11 kA m^{-2}.

Figure 7 compares J-V-L-characteristics of single-layer, bilayer and triple-layer devices using PPyrTPA as emitting material. Bilayer and triple-layer devices were fabricated in the following sandwich structures: ITO/PEDOT:PSS/TFB/PPyrTPA/Ca/Al and ITO/PEDOT:PSS/TFB/PPyrTPA/PEGPF/Ca/Al, respectively. All pyrene-based devices exhibited a deep-blue electroluminescence emission achieving maximum luminance values of 2924 cd m^{-2} for the single-layer device, 7817 cd m^{-2} for the bilayer device and 16 540 cd m^{-2} for the triple-layer PLED. Compared to the PPyrTPA-single layer device this means a more than 2.5-fold and more than 5.6-fold enhancement, respectively, of the maximum luminance for the bilayer device and for the triple-layer PLED. The enhancement of the devices' overall performance also reflected itself in the reduction of the onset voltage from 4.4 V in the single layer PLED to 3.9 V for the triple-layer assembly. By the application of TFB as HTL into the assembly the maximum LE could be raised from 0.27 cd A^{-1} to 0.43 cd A^{-1}. Additional insertion of PEGPF as ETL led to a maximum luminous efficiency of 1.42 cd A^{-1} for the triple-layer device. EL-spectra of the multilayer (bilayer- and triple-layer) PLEDs are presented in the insets of Figure 7b and Figure 7c, respectively. Both show a deep-blue emission in the same range as PPyrTPA single-layer devices (CIE1931: $x = 0.157$, $y = 0.174$; $x = 0.163$, $y = 0.216$). More importantly, a comparison of these emission characteristics to the EL-spectra of the TFB- (inset Figure 6a) and PEGPF-(inset Figure 6b) single-layer PLEDs shows that no EL contribution of the transporting materials can be detected which evidences that the EL-emission stems exclusively from PPyrTPA. These results (summarized in Table 1) demonstrate the improvement of PPyrTPA-based PLEDs by the application of the triple-layer assembly. The following causes are responsible for the enhancement of the PLEDs performance. In case of the bilayer device firstly the insertion of TFB leads to a stepwise reduction of the hole injection barrier between the Fermi-level of PEDOT:PSS and the VBM of PPyrTPA enabling an improved hole injection. Secondly, as shown by the UPS measurements, a pronounced energy barrier is formed between the PPyrTPA and TFB CBM levels, blocking electrons at that interface and inhibiting their extraction from the EML. For the triple-layer PLED UPS results revealed that the incorporation of PEGPF leads to the generation of an additional barrier for holes at the cathode side of PPyrTPA. Due to the VBM offset between

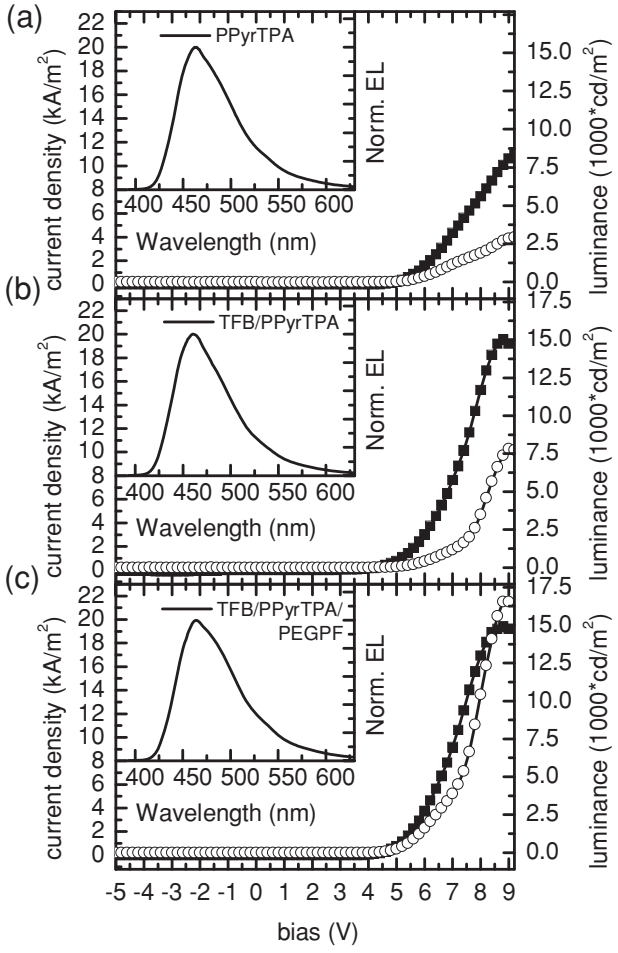

Figure 7. J-V-L-characteristics of single-layer, bilayer and triple-layer devices using PPyrTPA as emitting material. Current density (line with squares)/luminance (line with circles) as a function of the bias voltage in a) an ITO/PEDOT:PSS/PPyrTPA/Ca/Al device, b) an ITO/PEDOT:PSS/TFB/PPyrTPA/Ca/Al device using TFB as a hole injection layer, c) in an ITO/PEDOT:PSS/TFB/PPyrTPA/PEGPF/Ca/Al device with TFB as HTL and PEGPF as an ETL. The insets show the electroluminescence emission spectra of the same devices at a current density of 1.11kA m^{-2} and at a bias of 5.7, 5.2, and 5.1 V, respectively.

PPyrTPA and PEGPF the extraction of holes from the EML is hindered significantly. The formation of these barriers consequently leads to an enhanced charge carrier density within the EML which induces an increased exciton formation probability within the EML resulting in higher luminance and luminous efficiency values for the bilayer PLED and even more for the triple-layer device. Please note that, as reported by Kim et al.,[38] an oxidative doping of the emissive layer at the PEDOT:PSS/EML-interface is able to reduce the luminescence efficiency of a device significantly. Hence it is very likely that the spatial separation of PEDOT:PSS and PPyrTPA by TFB plays a decisive role for the enhancement of the LE in the bilayer and the triple-layer devices. With respect to the lifetime of the as presented bilayer and triple-layer devices, it is important to note that during their characterization all devices exhibited a good spectral stability over several tens of hours. The devices have

not yet been tested beyond that time; however, their lifetime is expected to be in the same range as for other typically blue emitting PLEDs.

Compared to already reported results, the utilization of TFB–stabilized by thermal treatment–as an HTL in PLEDs resulted in similar relative enhancement to the device performance as presented in previous work.[15] In addition, a comparison of the results presented in this current work to those achieved by Sax et al.,[13] using a similar polar soluble fluorene based polymer, suggests that PEGPF is also suitable as ETL for other commonly used polymers like polyfluorene or polyindenofluorene. With respect to the luminous efficiency, its enhancement or the maximum luminance values, respectively, the performance of the as presented triple layer device even superseded previous works using polar soluble polyfluorenes as ETL or athracene-based polymers as blue emitters.[13,39] Yet, the herein presented LEs stayed moderate compared to the work published by Tseng et al.,[40] where a liquid buffer method was used, or even more important compared to the single layer devices presented by Huang et al.[41] Nevertheless, to the best of our knowledge, the results presented in this work are among the best for conceptual studies on blue emitting solution processed PLEDs with more than two polymer layers and realized without the use of any crosslinking agents or buffer liquids.

For future work, however, at least an efficiency beyond 5 cd A^{-1} for blue emitting devices has to be the goal to aim for in order to exploit the advantages of solution based processing techniques. Therefore, improved hole and electron transport materials will be tested in a multilayer assembly in order to reach that goal with PPyrTPA as emitting material, whereby especially the performance limiting charge injection barriers between charge transport layers and the EML have to be reduced. Moreover, low workfunction metals like Li or Cs, their fluorides or carbonates, respectively, could be used as cathode materials, providing an ohmic contact and thus further enhance the overall device efficiency.

3. Conclusions

We presented the realization of a fully solution-processed triple-layer polymer light-emitting diode. A successive deposition of the individual organic layers without a redissolving of an already present layer was realized by two strategies. Firstly, for the hole injection polymer, a layer stabilization was achieved by thermal treatment making the material insoluble for non-polar solvents, thus enabling the deposition of the next, i.e., the emissive layer from a non-polar solution. Secondly, for the application of a third layer, an orthogonal solvent approach was applied. For that purpose, a new polyfluorene polymer was designed, bearing polyethylene glycol side chains. The specific molecular design of this polymer ensures the polymer's solubility in polar solvents and facilitates electron injection into the device. Layer-by-layer AFM-investigations of an assembly comprising the structure ITO/PEDOT:PSS/TFB/PPyrTPA/PEGPF revealed that the presented approach allows non-erosive sequential deposition of different polymers on top of each other. UPS measurements demonstrated that the chosen combination of materials exhibits a favorable energy-level alignment forming pronounced energy barriers for electrons and holes at the EML/HTL- and EML/ETL-interface, respectively. Thereby charge carrier confinement is generated within the emitting layer of a triple-layer PLED. These findings resulted in solution-processed triple-layer PLEDs with deep blue electroluminescence emission from the pyrene-based emitting material and significantly enhanced efficiencies as a consequence of improved exciton formation probability in the EML. In particular, a maximum luminance of 16 540 cd m^{-2} and a maximum device efficiency of 1.42 cd A^{-1} were achieved, which constitutes a five-fold increase compared to single-layer devices. Future efforts will be made to test different hole- or electron transport polymers, in order to reduce charge injection limiting energy barriers between the EML and the transport layers and thus to further enhance the devices' luminous efficiency.

4. Experimental Section

Materials: Poly(9,9-dioctyl-fluorene-co-N-(4-butylphenyl)-diphenylamine) was purchased at Luminescence Technology Corp. (LUMTEC) and used without further purification. Poly(pyrene-co-TPA) was synthesized as reported elsewhere.[16]

General Details: ^{1}H and ^{13}C NMR spectra were recorded on a Bruker AMX 300 NMR (300 and 75 MHz, respectively) with dichloromethane-d2 or THF-d8 as solvents and the solvent signal as internal standards. Melting points were determined on a Büchi hot-stage apparatus and are not corrected. FD mass spectra were performed with a VG-Instruments ZAB 2-SE-FDP. Matrix-assisted laser desorption/ionization time-of-flight (MALDI-TOF) analysis was carried out using a Bruker Time-of-Flight MS Reflex III instrument and a dithranol matrix with DCM as solvent. Gel permeation chromatography (GPC) was performed with PSS-SDV columns (SDV = styrol-divinylbenzol-copolymer; three columns, pore widths 500, 105, and 106 A) connected with UV–Vis/refractive index (RI) detector. THF was used as solvent. The calibration was based on polystyrene standards. The elemental analyses were carried out by the Microanalytical Laboratory of Johannes Gutenberg University.

The starting material 2,7-dibromo-9,9-di(pent-4-yn-1-yl)-9H-fluorene (Alkynyl-Fln) was prepared in analogy to a former reported route.[42] 3,4-Bis(4-methoxyphenyl)-2,5-diphenylcyclopenta-2,4-dienone ($CP(OMe)_2$) was prepared as described by K. R. J. Thomas.[43] Methyl and bromo endcapped polyethylene glycol 750 (CH_3-PEG-Br(750)) was purchased from Rapp Polymere. All other reagents and solvents were purchased from Sigma-Aldrich in the highest purity grade.

Synthesis of 9,9-bis(3-(5′,6′-bis(4-methoxyphenyl)-[1,1′:4′,1″-terphenyl]-2′-yl)propyl)-2,7-dibromo-fluorene (Monomer A): The starting materials Alkynyl-Fln (700 mg, 1.53 mmol) and $CP(OMe)_2$ (1.501 g, 3.38 mmol) were dissolved in *o*-Xylene (8 mL) in a microwave reaction glass tube. After being flushed with argon for 10 min, the mixture was heated in a microwave reactor to 170 °C (max. power 300 W, max. pressure 11 bar) for 12 h. The solvent was evaporated to give a brown crude product which was purified by silica column chromatography (gradient DCM/Hexane 2/1 → DCM). The final product was obtained as an off-white powder (1.69 g, 85%). ^{1}H NMR (300 MHz, CD_2Cl_2) δ = 7.53–7.45 (m, 4 H, Aryl), 7.27 (s, 4 H, Aryl), 7.18–7.11 (m, 12 H, Aryl), 7.06–7.02 (m, 6 H, Aryl), 6.76–6.73 (dd, 4 H, Aryl), 6.67–6.58 (dd, 4 H, Aryl), 6.44–6.34 (dd, 4 H, Aryl), 3.61 (s, 6 H, OMe), 3.57 (s, 6 H, OMe), 2.22–2.17 (t, 4 H), 1.75–1.69 (m, 4 H), 0.66–0.64 (m, 4 H); ^{13}C NMR (75 MHz, CD_2Cl_2) δ = 157.88, 157.56, 152.53, 142.89, 141.92, 141.33, 141.20, 140.76, 139.76, 139.68, 138.14, 133.62, 133.20, 133.10, 132.74, 130.89, 130.69, 130.50, 130.42, 128.07, 127.84, 126.67, 126.52, 122.22, 121.81, 112.75, 112.39, 55.97, 55.41, 55.35, 40.62, 34.75, 26.27; FD-MS: m/z = 1287.8 [M^+]; MALDI-TOF (Dithranol): m/z = 1288.7 g mol^{-1}; m.p. = 156–160 °C; EA found 77.21% C, 5.60% H–calculated 77.32% C, 5.31% H.

Synthesis of 9,9-Bis(3-(5′,6′-bis(4-methoxyphenyl)-[1,1′:4′,1″-terphenyl]-2′-yl)propyl)-9′,9′-dioctyl-2,7-polyfluorene (MeO-PF): Monomer A (150 mg, 0.233 mmol) and Monomer B (300 mg, 0.233 mmol) were dissolved in toluene (10 mL) and a 40% solution of tetraethylammonium hydroxide in water (2 mL) was added. The oxygen was removed via freeze-pump-thaw technique (3×) prior to the addition of the catalyst $Pd(PPh_3)_4$ (5.4 mg, 0.0023 mmol). After an additional freeze-pump-thaw cycle, the mixture was heated to 90 °C for 16 h.The first endcapping agent phenylboronic acid pinacol ester was added from a stock solution (50 g L^{-1}, 0.5 mL, 0.117 mmol) and the reaction was continued for 2 h. Then bromobenzene (35 mg, 0.233 mmol) was added as the second endcapping agent. After 2 h, the mixture was allowed to cool to room temperature and precipitated from methanol. After filtration, the product was redissolved in CH_2Cl_2, filtered through a 0,2 µm pore syringe filter and reprecipitated from methanol. After drying in high vacuum, an off-white powder was obtained (325 mg, 92%). GPC (THF): M_n = 15 000, M_w = 35 000, *PD* = 2.33; ^{1}H NMR (300 MHz, CD_2Cl_2) δ = 7.92-7.66 (m, 12 H, Aryl), 7.57-6.29 (m, 38 H, Aryl), 3.59 (s, 6 H, OMe), 3.51 (s, 6 H, OMe), 2.27–1.98 (bm, 12 H), 1.27-1.09 (bm, 22 H), 0.82-0.78 (bm, 12 H); ^{13}C NMR (75 MHz, CD_2Cl_2) δ = 157.87, 157.53, 152.52, 142.92, 141.87, 141.31, 141.21, 140.84, 140.10, 138.07, 133.63, 133.29, 133.13, 132.72, 130.70, 130.45, 128.03, 127.72, 126.85, 126.49, 122.04, 120.59, 112.75, 112.40, 55.40, 55.40, 55.27, 54.56, 54.20, 54.00, 53.84, 53.28, 32.44, 30.62, 29.85, 23.24, 14.50.

Synthesis of 9,9-bis(3-(5′,6′-bis(4-hydroxyphenyl)-[1,1′:4′,1″-terphenyl]-2′-yl)propyl)-9′,9′-dioctyl-2,7-polyfluorene (OH-PF): MeO-PF (135 mg, 0.089 mmol) was dissolved in dry CH_2Cl_2 and cooled to 0 °C. Then, a solution of BBr_3 in CH_2Cl_2 (1 M, 0.54 mL, 0.54 mmol) was added. After 1 h the cooling was removed. The mixture was stirred for 16 h during which a dark precipitate formed. The reaction was quenched by several drops of water turning the precipitate yellow within a minute. The solvent was evaporated under reduced pressure. The residue was dissolved in THF and precipitated from methanol. After reprecipitation (THF to methanol) the product was collected via centrifugation and dried in high vacuum to yield a yellow to greenish solid (96 mg, 74%). GPC (DMF): M_n = 23200, M_w = 45000, *PD* = 1.94. ^{1}H NMR (300 MHz, [D_8]-THF) δ = 7.94–7.55 (m, 16 H), 7.04–6.78 (m, 22 H), 6.50–6.42 (dd, 8 H), 6.25-6.14 (dd, 8 H), 2.27–1.94 (bm, 12 H), 1.51–0.77 (bm, 34 H); ^{13}C NMR (75 MHz, [D_8]–THF) δ = 156.25, 155.90, 152.85, 152.36, 143.86, 142.75, 141.86, 141.73, 141.48, 140.14, 139.01, 133.56, 133.15, 132.82, 132.43, 131.24, 130.87, 128.29, 128.09, 127.40, 126.66, 122.23, 120.99, 114.80, 114.49, 56.51, 56.20, 41.35, 35.78, 32.94, 31.10, 30.30, 23.67, 14.68.

Synthesis of 9,9-bis(3-(5′,6′-bis(4-(polyethylene glycol)phenyl)-[1,1′:4′,1″-terphenyl]-2′-yl)propyl)-9′,9′-dioctyl-2,7-polyfluorene (PEGPF): OH-PF (50 mg, 0.034 mmol) was dissolved in THF under argon and was treated with KOH (16 mg, 0.239 mmol) and CH_3-PEG-Br(750) (192 mg, ca. 0.24 mmol). The mixture was heated for 3 days to 65 °C. The solvent was evaporated under reduced pressure and the residue was dissolved in CH_2Cl_2. The undissolved residue (KBr and KOH) was filtered off through a 5 µL pore syringe filter. The solution was concentrated in vacuo after which it was added dropwise to hexane. The precipitated waxy solid was air dried and washed extensively with water. Finally, the product was redissolved in CH_2Cl_2 and reprecipitated from hexane. For device applications, it was purified via recycling GPC using chloroform as the eluent (85 mg, 57%). GPC (DMF): M_n = 48 200, M_w = 143 600, *PD* = 2.98; ^{1}H NMR (300 MHz, CD_2Cl_2) δ = 7.89–6.24 (bm, 50 H, Aryl), 3.88–3.33 (bm, 173 H, O-CH_2-CH_2-O), 2.38–1.90 (bm, 8 H), 1.29–0.77 (bm, 38 H); ^{13}C NMR (75 MHz, CD_2Cl_2) δ = 156.96, 156.62, 152.49, 142.84, 141.78, 141.25, 140.83, 140.12, 138.00, 133.14, 132.75, 130.70, 130.43, 128.02, 127.69, 126.44, 120.64, 114.49, 114.15, 113.34, 112.98, 72.93, 72.49, 71.23, 71.08, 70.95, 70.13, 69.28, 67.46, 64.89, 63.92, 59.19, 56.09, 37.64, 33.31, 32.42, 30.59, 30.26, 29.79, 29.10, 27.63, 26.26, 23.21, 14.52.

Surface Morphology: For AFM-investigations first of all indium tin oxide covered glass substrates were cleaned mechanically by the use of acetone and isopropanol. The substrates were subjected to subsequent supersonic cleaning steps in deionized water, toluene and isopropanol. Prior to the depostition of poly(3,4-ethylenedioxythiophene)–polystyrenesulfonic acid (CLEVIOS P VP AI 4083) (PEDOT:PSS) from Heraeus as a first polymeric layer, to enhance the wettability of PEDOT:PSS on the substrate, the ITO substrates were subdued to a dry cleaning procedure in oxygen plasma. PEDOT:PSS was spin-cast onto the as prepared substrates under ambient conditions and dried according to the specifications under dynamic vacuum with a pressure less than 1×10^{-5} mbar. TFB layers were deposited by spin-coating from xylene solution (15 mg mL^{-1}) under inert conditions and dried in argon at 200 °C for 2 h. Afterwards, the substrates were cooled to room temperature on a cold surface. To remove the soluble parts of the annealed polymer the TFB layer was spin-rinsed by pure toluene resulting in a final layer thickness of 5 nm with good reproducibility as long as annealing temperature and time were kept constant. PPyrTPA layers were spin-cast onto prepared TFB films from an 8 mg mL^{-1} toluene solution and dried at 80 °C for 2 h in vacuum ($p \leq 1 \times 10^{-5}$ mbar) resulting in layer thicknesses of 50 nm. Prior to depositing PEGPF, the TFB/PPyrTPA-substrates were spin-rinsed by pure methanol. Afterwards PEGPF dissolved in methanol and a polymer content of 1 mg mL^{-1} was applied by spin-coating. The layer was annealed at 70 °C for 1 h under high vacuum ($p \leq 1 \times 10^{-5}$ mbar) and exhibited a thickness of 10 nm, which was well controllable for spinning speeds above 1500 rpm. After each deposition and the accompanied annealing procedures the surface morphology and layer thicknesses were measured at several positions on an analogously assembled reference-substrate in tapping mode by a Veeco Dimension V atomic force microscope equipped with a Nanoscope V controller.

UPS Measurements: For UPS studies, polymers were deposited and annealed the same way as described for AFM-sample preparation. UPS measurements were performed at the endstation SurICat (beamline PM4) of the synchrotron light source BESSY II (Berlin, Germany). Spectra were collected with a hemispherical electron energy analyzer (Scienta SES 100). The excitation photon energy was 35 eV and the energy resolution 150 meV. SECO spectra to determine the sample work function were recorded while the sample was biased at -10 V to clear the analyzer work function. To assure the absence of sample charging standard procedures including variation of the excitation, photon flux and sample illumination with visible light were applied for every sample. An error of less than ± 0.1 eV is estimated for reported energy values.

PLED Fabrication and Characterization: For the fabrication of single- and multilayer-devices the respective polymer layers of TFB, PPyrTPA and PEGPF were deposited on a 50 nm PEDOT:PSS film covering ITO which was prepared the same way as for AFM-samples, whereby after the annealing of PEDOT:PSS all processes where performed under inert conditions. For single layer PLEDs TFB was applied by spin coating from a 6 mg mL^{-1} solution in xylene, PPyrTPA was spin cast from an 8 mg mL^{-1} toluene solution and the spin coating of PEGPF was performed with the polymer being dissolved in methanol with a concentration of 6 mg mL^{-1}. After spin coating, the samples were annealed for 1 h under high vacuum ($p \leq 1 \times 10^{-5}$ mbar) at 120 °C in the case of TFB and PPyrTPA and at 70 °C when PEGPF was used. The thicknesses of the respective polymer layers were determined to 50 nm with a mean error of less than 10%. To fabricate bilayer- and triple-layer-PLEDs all organic layers were deposited analogously to the procedures presented above for AFM-samples. After polymer deposition 10 nm of Ca and 100 nm Al as cathode, materials were deposited thermally through a shadow mask forming a device area of 9 mm^2 in a custom made vapor deposition unit from tungsten boats at an initial base pressure less than 1×10^{-6} mbar. Current–luminance–voltage (I–L–V) characteristics were recorded in a customized setup. To determine the I–V characteristics, a Keithley 2612A source measure unit was used and a Keithley 6485 Picoammeter using a calibrated photodiode to record the luminance. For each single- or multilayer device configuration, a series of 18 devices was investigated. Device efficiencies exhibited a mean variation of less than 15%. Electroluminescence (EL) spectra were acquired using an ORIEL spectrometer with a calibrated charge-coupled device (CCD) camera attached to it.

Supporting Information

Supporting Information is available from the Wiley Online Library or from the author.

Acknowledgements

R.T. gratefully acknowledges financial support by the Christian Doppler Research Association, the Austrian Federal Ministry of Economy, Family and Youth (BMWFJ), and ISOVOLTAIC AG. Work in Berlin was supported by the DFG (SFB951) and the EC (HYMEC, GENIUS).

Received: January 29, 2013
Revised: March 8, 2013
Published online: April 22, 2013

[1] J. H. Burroughes, D. D. C. Bradley, A. R. Brown, R. N. Marks, K. Mackay, R. H. Friend, P. L. Burns, A. B. Holmes, *Nature* **1990**, *347*, 539.
[2] M. Nikam, R. Singh, S. Bhise, *IJCA Proceedings on International Conference on Advances in Communication and Computing Technologies* **2012**, 31.
[3] R. Friend, R. Gymer, A. Holmes, J. H. Burroughes, R. N. Marks, C. Taliani, D. D. C. Bradley, D. A. Dos Santos, J.-L. Brédas, M. Lögdlund, W. R. Salaneck, *Nature* **1999**, *397*, 121.
[4] S. Tasch, E. J. W. List, O. Ekström, W. Graupner, G. Leising, P. Schlichting, U. Rohr, Y. Geerts, U. Scherf, K. Müllen, *Appl. Phys. Lett.* **1997**, *71*, 2883.
[5] G. G. Malliaras, J. C. Scott, *J. Appl. Phys.* **1998**, *83*, 5399.
[6] L. Duan, L. Hou, T.-W. Lee, J. Qiao, D. Zhang, G. Dong, L. Wang, Y. Qiu, *J. Mater. Chem.* **2010**, *20*, 6392.
[7] W.-C. Lin, W.-B. Wang, Y.-C. Lin, B.-Y. Yu, Y.-Y. Chen, M.-F. Hsu, J.-H. Jou, J.-J. Shyue, *Org. Electron.* **2009**, *10*, 581.
[8] C. A. Zuniga, S. Barlow, S. R. Marder, *Chem. Mater.* **2011**, *23*, 658.
[9] W. Li, Q. Wang, J. Cui, H. Chou, S. E. Shaheen, G. E. Jabbour, J. Anderson, P. Lee, B. Kippelen, N. Peyghambarian, N. R. Armstrong, T. J. Marks, *Adv. Mater.* **1999**, *11*, 730.
[10] Y.-H. Niu, M. S. Liu, J.-W. Ka, J. Bardeker, M. T. Zin, R. Schofield, Y. Chi, A. K.-Y. Jen, *Adv. Mater.* **2007**, *19*, 300.
[11] Y.-J. Cheng, M. S. Liu, Y. Zhang, Y. Niu, F. Huang, J.-W. Ka, H.-L. Yip, Y. Tian, A. K.-Y. Jen, *Chem. Mater.* **2008**, *20*, 413.
[12] F. Huang, H. Wu, Y. Cao, *Chem. Soc. Rev.* **2010**, *39*, 2500.
[13] S. Sax, N. Rugen-Penkalla, A. Neuhold, S. Schuh, E. Zojer, E. J. W. List, K. Müllen, *Adv. Mater.* **2010**, *22*, 2087.
[14] J.-S. Kim, R. H. Friend, I. Grizzi, J. H. Burroughes, *Appl. Phys. Lett.* **2005**, *87*, 023506.
[15] S.-R. Tseng, S.-Y. Li, H.-F. Meng, Y.-H. Yu, C.-M. Yang, H.-H. Liao, S.-F. Horng, C.-S. Hsu, *J. Appl. Phys.* **2007**, *101*, 084510.
[16] R. Trattnig, T. M. Figueira-Duarte, D. Lorbach, W. Wiedemair, S. Sax, S. Winkler, A. Vollmer, N. Koch, M. Manca, M. A. Loi, M. Baumgarten, E. J. W. List, K. Müllen, *Opt. Express* **2011**, *19*, A1281.
[17] G.-A. Wen, Y. Xin, X.-R. Zhu, W.-J. Zeng, R. Zhu, J.-C. Feng, Y. Cao, L. Zhao, L.-H. Wang, W. Wei, B. Peng, W. Huang, *Polymer* **2007**, *48*, 1824.
[18] K. H. Lee, L. K. Kang, Y. S. Kwon, J. Y. Lee, S. Kang, G. Y. Kim, J. H. Seo, Y. K. Kim, S. S. Yoon, *Thin Solid Films* **2010**, *518*, 5091.
[19] H. Kim, N. Schulte, G. Zhou, K. Müllen, F. Laquai, *Adv. Mater.* **2011**, *23*, 894.
[20] S. Setayesh, D. Marsitzky, K. Müllen, *Macromolecules* **2000**, *33*, 2016.
[21] J. Jacob, S. Sax, M. Gaal, E. J. W. List, A. C. Grimsdale, K. Müllen, *Macromolecules* **2005**, *38*, 9933.
[22] J. Ding, Y. Tao, M. Day, J. Roovers, M. D Iorio, *J. Opt. A: Pure Appl. Opt.* **2002**, *4*, S267.
[23] H. Scheiber, M. Graf, H. Plank, E. Zojer, C. Slugovc, S. Kappaun, F. Galbrecht, U. Scherf, E. J. W. List, *Adv. Funct. Mater.* **2008**, *18*, 2480.
[24] X. Gong, D. Moses, A. J. Heeger, S. Xiao, *Synth. Met.* **2004**, *141*, 17.
[25] T. M. Figueira-Duarte, P. G. Del Rosso, R. Trattnig, S. Sax, E. J. W. List, K. Müllen, *Adv. Mater.* **2010**, *22*, 990.
[26] M. Redecker, D. D. C. Bradley, M. Inbasekaran, W. W. Wu, E. P. Woo, *Adv. Mater.* **1999**, *11*, 241.
[27] X. Y. Deng, W. M. Lau, K. Y. Wong, K. H. Low, H. F. Chow, Y. Cao, *Appl. Phys. Lett.* **2004**, *84*, 3522.
[28] Y.-H. Niu, H. Ma, Q. Xu, A. K.-Y. Jen, *Appl. Phys. Lett.* **2005**, *86*, 083504.
[29] F. Huang, Y.-H. Niu, Y. Zhang, J.-W. Ka, M. S. Liu, A. K.-Y. Jen, *Adv. Mater.* **2007**, *19*, 2010.
[30] W.-F. Su, R.-T. Chen, Y. Chen, *J. Polym. Sci. Part A: Polym. Chem.* **2011**, *49*, 352.
[31] X. Xu, B. Han, J. Chen, J. Peng, H. Wu, Y. Cao, *Macromolecules* **2011**, *44*, 4204.
[32] M. S. Liu, Y.-H. Niu, J.-W. Ka, H.-L. Yip, F. Huang, J. Luo, T.-D. Kim, A. K.-Y. Jen, *Macromolecules* **2008**, *41*, 9570.
[33] S. Setayesh, A. C. Grimsdale, T. Weil, V. Enkelmann, K. Müllen, F. Meghdadi, E. J. W. List, G. Leising, *J. Am. Chem. Soc.* **2001**, *123*, 946.
[34] W. Hild, A. Opitz, J. A. Schaefer, M. Scherge, *Wear* **2003**, *254*, 871.
[35] J. Hwang, E. Kim, J. Liu, J.-L. Bredas, A. Duggal, A. Kahn, *J. Phys. Chem. C* **2007**, *111*, 1378.
[36] G. Heimel, I. Salzmann, S. Duhm, J. P. Rabe, N. Koch, *Adv. Funct. Mater.* **2009**, *19*, 3874.
[37] U. Scherf, E. J. W. List, *Adv. Mater.* **2002**, *14*, 477.
[38] J.-S. Kim, P. K. H. Ho, C. E. Murphy, A. J. A. B. Seeley, I. Grizzi, J. H. Burroughes, R. H. Friend, *Chem. Phys. Lett.* **2004**, *386*, 2.
[39] H.-M. Shih, C.-J. Lin, S.-R. Tseng, C.-H. Lin, C.-S. Hsu, *Macromol. Chem. Phys.* **2011**, *212*, 1100.
[40] S.-R. Tseng, H.-F. Meng, C.-H. Yeh, H.-C. Lai, S.-F. Horng, H.-H. Liao, C.-S. Hsu, L.-C. Lin, *Synth. Met.* **2008**, *158*, 130.
[41] C.-W. Huang, K.-Y. Peng, C.-Y. Liu, T.-H. Jen, N.-J. Yang, S.-A. Chen, *Adv. Mater.* **2008**, *20*, 3709.
[42] N. Rugen-Penkalla, M. Klapper, K. Müllen, *Macromolecules* **2012**, *45*, 2301.
[43] K. R. J. Thomas, M. Velusamy, J. T. Lin, C. H. Chuen, Y.-T. Tao, *J. Mater. Chem.* **2005**, *15*, 4453.